

A Functional Approach To Uncover the Low-Temperature Adaptation Strategies of the Archaeon *Methanosarcina barkeri*

Eoin Gunnigle,^a Paul McCay,^a Matthew Fuszard,^b Catherine H. Botting,^b Florence Abram,^a Vincent O'Flaherty^a

Microbial Ecology Laboratory, Microbiology, School of Natural Sciences, and Ryan Institute, National University of Ireland, Galway, Ireland^a; BSRC Mass Spectrometry and Proteomics Facility, Biomedical Sciences Research Complex, North Haugh, University of Saint Andrews, Fife, Scotland, United Kingdom^b

Low-temperature anaerobic digestion (LTAD) technology is underpinned by a diverse microbial community. The methanogenic archaea represent a key functional group in these consortia, undertaking CO₂ reduction as well as acetate and methylated C₁ metabolism with subsequent biogas (40 to 60% CH₄ and 30 to 50% CO₂) formation. However, the cold adaptation strategies, which allow methanogens to function efficiently in LTAD, remain unclear. Here, a pure-culture proteomic approach was employed to study the functional characteristics of *Methanosarcina barkeri* (optimum growth temperature, 37°C), which has been detected in LTAD bioreactors. Two experimental approaches were undertaken. The first approach aimed to characterize a low-temperature shock response (LTSR) of *M. barkeri* DSMZ 800^T grown at 37°C with a temperature drop to 15°C, while the second experimental approach aimed to examine the low-temperature adaptation strategies (LTAS) of the same strain when it was grown at 15°C. The latter experiment employed cell viability and growth measurements (optical density at 600 nm [OD₆₀₀]), which directly compared *M. barkeri* cells grown at 15°C with those grown at 37°C. During the LTSR experiment, a total of 127 proteins were detected in 37°C and 15°C samples, with 20 proteins differentially expressed with respect to temperature, while in the LTAS experiment 39% of proteins identified were differentially expressed between phases of growth. Functional categories included methanogenesis, cellular information processing, and chaperones. By applying a polyphasic approach (proteomics and growth studies), insights into the low-temperature adaptation capacity of this mesophilically characterized methanogen were obtained which suggest that the metabolically diverse *Methanosarcinaceae* could be functionally relevant for LTAD systems.

Archaea are ubiquitous in low-temperature habitats such as polar marine waters (1, 2), alpine lakes (3), permafrost (4), and glacier ice (5). Methanogens represent the most characterized psychrophilic archaeal group (6). As such, low-temperature methanogenesis has been the focus of many studies, such as those focusing on measuring the methanogenic contribution to the global warming of cold areas (7) and also those using an astrobiological approach, where the ability of methanogens to survive under cold anoxic conditions has made them candidates as Earth analogues for extraterrestrial life (8).

Low-temperature methanogenic activity is also important from a biotechnological viewpoint, such as its application in low-temperature anaerobic digestion (LTAD) (9). Evidence of efficient LTAD treatment of wastewaters has been recorded in laboratory-scale trials which directly compared low-temperature bioreactor performance (chemical oxygen demand removal [COD] and biogas production) with traditional mesophilic configurations (10, 11). Experiments which comprised an initial mesophilic (37°C) bioreactor operation phase followed by a decrease to low-temperature conditions ($\leq 15^\circ\text{C}$) have also been undertaken (12, 13). In these studies, low-temperature bioreactors achieved comparable performance levels to mesophilic systems after an initial period of "adaptation." As a mesophilic inoculum was used to seed these bioreactors, a psychrotolerant capacity was deemed to be evident in the mixed microbial consortia underpinning these bioreactors. However, there still remains a significant knowledge gap relating to low-temperature methanogenic adaptation strategies, which require further elucidation for the optimization of LTAD systems.

There are three primary modes of methanogenic metabolism based on CO₂ reduction, acetate decarboxylation, and methylotrophic activity (e.g., reduction of methylamines). Acetoclastic

(acetate decarboxylation) methanogenesis has been recorded as being an important methanogenic pathway in low-temperature environments, including bioengineered systems (14). The order *Methanosarcinales* includes the only two known acetoclastic families, the *Methanosaetaceae* and the *Methanosarcinaceae*. The former have been historically categorized as strict acetoclastic methanogens although a recent genomic study highlighted the metabolic capacity for possible methyl group oxidation in three sequenced *Methanosaetaceae* strains (15). Nevertheless, this group has a minimum threshold concentration of 7 to 70 μM acetate (16) and has been documented to outcompete *Methanosarcinaceae* in environments where acetate concentrations are low (17, 18). However, in addition to acetate, the *Methanosarcinaceae* have the ability to utilize methylated compounds such as methanol and methylamines, with some species also able to use H₂/CO₂ as a carbon and energy source.

In many LTAD studies, *Methanosaetaceae* have been the predominant acetoclastic methanogenic group, with their abundance positively correlated to process efficiency (19–21) and granular sludge integrity (14). In contrast, low levels of *Methanosarcinaceae* have been found in well-functioning LTAD systems (14, 22). For example, in one study this group was detected below the quantification limit of the 16S rRNA gene assay, whereas *Methanosaetaceae* comprised 75% of total measured methanogenic 16S rRNA

Received 7 December 2012 Accepted 14 April 2013

Published ahead of print 3 May 2013

Address correspondence to Eoin Gunnigle, e.gunnigle1@nuigalway.ie.

Copyright © 2013, American Society for Microbiology. All Rights Reserved.

doi:10.1128/AEM.03787-12

TABLE 1 Overview of *M. barkeri* growth characteristics

Parameter	Value of the parameter by expt and time (days) ^a													
	LTAS at 37°C				LTAS sampling at 15°C								LTSR at:	
	0.8	1.8	3.7	7	I	II	III	IV	37°C	15°C				
OD ₆₀₀	0.53	0.56	2.13	1.35	0.05	0.31	0.25	0.23	0.21	0.24	0.35	0.76	1.92	0.84
% CH ₄	1.8	19	46	43	1.2	1.9	2	3.7	6.7	15.6	25	46	58	46

^a H₂/CO₂ plus methanol was used as the substrate. LTAS, low-temperature adaptation strategies; LTSR, low-temperature shock response; I to IV, LTAS sampling points for iTRAQ analysis.

gene concentrations (23). However, a marked increase in *Methanosarcinaceae* signatures has been recorded during periods of bioreactor instability brought about through changes in operational parameters, e.g., temperature (14) and hydraulic retention time (24), with acetate accumulation apparent during this period. This would suggest that *Methanosarcinaceae* have the metabolic capacity to survive at low cell levels within a well-functioning LTAD system, where acetate concentrations are kept low. Thereafter, through a perturbation event this group can proliferate (acetate accumulation above utilization threshold). Thus, *Methanosarcinaceae* may have an important role in LTAD by ensuring a certain level of process stability during transient operation periods (11, 25).

The *Methanosarcinaceae* species *Methanosarcina barkeri* is a metabolically versatile methanogen which can grow on H₂/CO₂, methanol, various methylamines, and acetate as carbon and energy sources (26). This species has previously been the focus of a variety of studies, including growth experiments (27, 28), genomic investigations (29, 30), and enzymatic characterization (31, 32). In the present study, we employed a systematic, proteomics-based approach to characterize the low-temperature adaptive strategies of the methylotrophic *M. barkeri* strain DSMZ 800^T, which was isolated from an anaerobic digester. Our hypothesis was that the organism would display an adaptive capacity to allow growth through the utilization of methanol and/or H₂/CO₂ under low-temperature conditions, thereby providing insights into the acetate-independent psychrotolerant growth and function of a *Methanosarcina* sp., which could be related to survival mechanisms employed by environmental strains in LTAD systems.

MATERIALS AND METHODS

Strain information, medium, and inoculum preparation. The archaeal strain *Methanosarcina barkeri* DSMZ 800^T (DSMZ, Braunschweig, Germany) was used throughout this study. Inoculum preparation was achieved using medium DMS 120 (pH 6.8) (33). After 40 ml of medium was added, each 60-ml vial was sealed with a butyl rubber bung and flushed with N₂/CO₂ (80:20, vol/vol) gas. Filter-sterilized reducing agents L-cysteine (2.5 mM) and Na₂S · 9H₂O (1.2 mM) were added after autoclaving as per DSMZ guidelines. In order to demonstrate that this strain was methylotrophic and to investigate substrate influence on growth, selected vials were supplemented with either methanol (156 mM; 50% [vol/vol] stock, filter sterilized), H₂/CO₂ (80:20, vol/vol), or methanol plus H₂/CO₂. Vials were inoculated with 2.5% (vol/vol) stock culture and incubated at 37°C on a shaker.

Batch culture setup. When cells reached stationary phase (optical density at 600 nm [OD₆₀₀] of ~2), inoculum was added anaerobically to fresh vials (for each substrate mix) to an OD₆₀₀ of ~0.05 in 40 ml of medium. Separate vials were then incubated at 15°C and 37°C for comparative analysis on a shaker. OD₆₀₀ measurements were taken at time

intervals for each temperature, while separate vials for headspace methane measurements (percent) (34) were run in parallel. This experiment aimed to give direct insights into the capacity of *M. barkeri* to adapt to low temperatures and will therefore be referred to as the low-temperature adaptation strategy (LTAS) study from this point on. Molecular analysis was carried out on samples from cultures fed with methanol plus H₂/CO₂ (Table 1), and for this purpose, cells from 40 ml of culture were harvested by flash-freezing with liquid nitrogen followed by storage at -80°C. Samples were then thawed and centrifuged at 8,000 × g for 10 min at 4°C. The supernatant was discarded, and the recovered biomass pellet (approximately 1.5 g of wet weight per sample) was stored at -80°C until use.

Continuous-culture setup. Continuous cultures of *M. barkeri* were established in a modified 500-ml Schott bottle (fitted with a three-port lid; Fisher Scientific) with a working volume of 400 ± 100 ml, connected to both medium and waste reservoirs. Anaerobic conditions were maintained in the vessel by sealing with butyl stoppers, by using gas-impermeable tubing connected to the medium reservoir, and by regularly flushing with N₂/CO₂ (80:20, vol/vol) gas. The sterile medium was allowed to acclimatize at 37°C overnight without shaking prior to inoculation with 2.5% (vol/vol) culture. The flow rate from the reservoir was controlled by a peristaltic pump (Watson-Marlow 205U) and was monitored and adjusted to maintain a steady dilution rate of 2.0 h⁻¹. The continuous-culture system was operated at 37°C, allowing a continuous culture to establish (3.5 days; OD₆₀₀ of ~1.9), after which point the temperature was dropped to 15°C. The system was further operated for 3.7 days (7.2 days of total running time). Samples for protein extraction (60 ml) were taken immediately before the temperature drop event and also at the end of the period of 15°C operation (Table 1). This experiment aimed to uncover the functional response of *M. barkeri* directly after a temperature drop to 15°C and will therefore be referred to as the low-temperature shock response (LTSR) experiment from this point on.

Cell viability measurements. The viability of cells during the LTAS experiment was investigated using a Live/Dead BacLight kit (Invitrogen) (35) (Table 1). Anaerobic conditions were maintained in samples during incubation with BacLight probes by sealing samples with N₂/CO₂ (80:20, vol/vol) gas. A Nikon Eclipse E600 epifluorescence microscope (Carl Zeiss, Oberkochen, Germany) was used to assess cell viability. Live cells were indicated by green fluorescence (BS2 filter; excitation, 450 to 490 nm; long-pass [LP] emission filter, 515 nm) while dead cells were indicated by red fluorescence (CY3 filter; excitation, 546 ± 12 nm; LP emission, 590 nm). Ten images of a microscope field (×100 magnification) were taken for each sample and visualized using QCapture Pro software.

Protein extraction and quantification. *M. barkeri* proteins were extracted from samples (Table 1) using a sonication method adapted from a previous LTAD proteomic study (36). Briefly, cell pellets were resuspended with 5 ml of noninterfering triethylammonium bicarbonate (TEAB) buffer. The cells were then disrupted by sonication (MSE Soniprep 150) at 40% amplitude for 30 s on ice. Fifteen pulses were applied with 30-s intervals to prevent thermal damage of cellular proteins. In order to remove any protein precipitates and cellular debris, lysates underwent centrifugation at 10,000 × g for 30 min at 4°C, and the resulting pellets were discarded. Protein precipitation from the supernatants was

achieved through incubation with ice-cold acetone (3:1, vol/vol) at -20°C for 1 h, after which the samples underwent centrifugation at $10,000 \times g$ for 15 min. The supernatants were discarded, and pellets were resuspended with 200 μl of TEAB buffer. Protein quantification was undertaken using a Calbiochem Non-Interfering Protein Assay kit (Merck KGaA, Darmstadt, Germany) by following the manufacturer's instructions.

iTRAQ labeling. For each study (LTAS and LTSR), replicate protein extracts from specified time points were used in an eight-plex iTRAQ (isobaric tags for relative and absolute quantification) labeling experiment (Table 1). One hundred micrograms of protein extract in 20- μl samples was labeled with iTRAQ reagents according to the manufacturer's guidelines (ABSciex, Foster City, CA). Briefly, each sample was reduced and denatured, and cysteine residues were blocked before digestion with 10 μl of 25 $\mu\text{g}/\mu\text{l}$ trypsin solution (1:20; Promega, Madison, WI) overnight at 37°C . The digested peptides were then labeled with iTRAQ tags as follows in the LTAS experiment: for duplicates of sample I, tags 113 and 114; for duplicates of sample II, tags 115 and 116; for duplicates of sample III, tags 117 and 118 tags; and for duplicates of sample IV, tags 119 and 121. For the LTSR experiment only four iTRAQ tags were required: for duplicate 37°C samples, tags 113 and 114; and for duplicate 15°C samples, tags 115 and 116. For each experimental setup, the samples were combined and subjected to peptide separation by cation exchange chromatography followed by liquid chromatography-tandem mass spectrometry (LC-MS/MS) analysis.

Cation exchange peptide separation and LC-MS/MS analysis. After trypsin digestion and labeling, peptides from individual samples were combined and resuspended in 1 ml of cation exchange loading buffer (10 mM KH_2PO_4 , pH 3.0, in 25% acetonitrile). The peptides were then separated by strong cation exchange chromatography on a PolySulfoethyl A column (PolyLC, Inc.) with an increasing salt gradient from 0 to 0.5 M over 30 min, and fractions were collected every 30 s. Fractions were pooled to give nine fractions of approximately equal peptide concentrations, as judged by inspection of the chromatogram, evaporated to dryness, and resuspended in 0.1% trifluoroacetic acid before desalting (PepClean C_{18} spin columns; ThermoScientific). Each fraction was further separated through reverse-phase chromatography directly before mass spectrometric analysis. This was achieved using an Eksigent nanoLC Ultra system coupled to a Nanoflex cHiPLC (ABSciex, Foster City, CA) equipped with a 200- μm by 0.5-mm ChromXP C_{18} -CL 3- μm , 120- \AA trap and 75- μm by 15-cm ChromXP C_{18} -CL 3- μm , 120- \AA column, using a gradient of increasing acetonitrile concentration containing 0.1% formic acid (15 to 40% acetonitrile in 40 min and 40 to 95% in a further 10 min, followed by 95% acetonitrile to clean the column). The eluent was sprayed into a TripleTOF 5600 mass spectrometer (ABSciex, Foster City, CA) and analyzed in information-dependent acquisition (IDA) mode, performing 0.25 s of MS followed by 2-s MS/MS analyses of the 20 most intense peaks seen by MS. These precursor masses were then excluded from analysis for the next 13 s. A rolling collision energy adjusted to 10 units higher than that normally used for peptides was employed to provide sufficient peptide fragmentation and generation of the iTRAQ reporter groups.

Two-dimensional gel electrophoresis (2-DGE). Eight two-dimensional (2-D) gels were run in total, corresponding to two duplicate independent extractions and two technical replicates from 37°C and 15°C LTAS samples, by following the protocol described in a previous study (36) (Table 1). Gel images were processed and analyzed with PDQuest-Advanced software, version 8.0.1 (Bio-Rad). Spot counts were obtained using the spot detection wizard enabling the Gaussian model option as recommended by the manufacturer. Ratios of spot intensities were determined for each sample. Protein expression ratios greater than 1.5-fold were considered significant. The 1.5-fold cutoff point for significance was based on the geometric standard deviation of the entire set of proteins identified (at least two unique peptides at $>99\%$ confidence), which has been used in many proteomic studies as a conservative cutoff for biological significance (37, 38). Proteins of interest were excised from the gels

and subjected to in-gel digestion prior to analysis using nanoflow liquid chromatography-electrospray ionization tandem mass spectrometry (nLC-ESI-MS/MS) (36).

Protein identification and quantification. The MS/MS data recovered from iTRAQ and 2-DGE LC-MS/MS were analyzed as follows: MS/MS data for +2 to +5 charged precursor ions which exceeded 150 cps were processed using the Paragon search algorithm (39) within the ProteinPilot, version 4.1, software program (ABSciex, Foster City, CA) against an internal database comprising the *M. barkeri* Fusaro genome (DSM 804, with 3,616 proteins in the UniProtKB database) along with potential contaminants (UniProtKB/Swiss-Prot database, accessed 19 June 2012). The data were searched using the following parameters: a detected protein threshold (unused ProtScore) of >0.05 , trypsin as the cleavage enzyme, one missed cleavage, iTRAQ modification of lysines and methyl methanethiosulfonate (MMTS) modification of cysteines as fixed modifications, and methionine oxidation selected as a variable modification. Peptide and protein lists were then exported from ProteinPilot to the ProteinPilot descriptive statistics template (PDST; ABSciex, Foster City, CA) for data management and additional analysis (e.g., Volcano and Quant false-discovery rate [FDR] worksheet). The FDR was calculated by ProteinPilot PDST using the embedded decoy search and was found to be $<2\%$ for all experiments.

RESULTS

Characteristics of *M. barkeri* grown at 37°C and 15°C . The levels of growth of *M. barkeri* at 37°C and 15°C were compared through OD_{600} measurements with different substrate mixes (methanol plus H_2/CO_2 , methanol alone, and H_2/CO_2 alone) (Fig. 1). The maximum specific growth rate (μ_{max}) was found to be dependent on both temperature and substrate (Table 2). The OD_{600} measurements indicated a minimal lag phase for cultures grown at 37°C , regardless of substrate, with an increase in the OD_{600} correlating with an increase in percent CH_4 production (Fig. 1). After a lag phase of ~ 1 day, growth at 15°C exhibited a similar profile to that observed at 37°C . On day 3, however, a long stationary phase was recorded prior to a further steady increase in growth from day 17. Although the μ_{max} was lower in the 15°C cultures, the cultures fed H_2/CO_2 plus methanol reached headspace percent CH_4 levels similar to those of their mesophilic counterparts, peaking at 70% CH_4 ($\pm 4.3\%$ standard error [SE]; $n = 3$) on day 41 of the incubation compared with 64% ($\pm 6.7\%$ SE; $n = 3$) on day 14 in 37°C vials (Fig. 1). The *M. barkeri* cultures with H_2/CO_2 as a sole substrate exhibited poor growth, and percent methane headspace values at both temperatures tested were lower than those of cultures fed with H_2/CO_2 plus methanol or with methanol only (Fig. 1). Although solubility of H_2 increases with decreasing temperature, difficulties with substrate delivery through gas input has been recorded previously (40). Also, as this was a methanol-adapted strain of *M. barkeri*, it is plausible that the metabolic capacity to reduce CO_2 using electrons from H_2 was thermodynamically unfavorable under submesophilic conditions, as suggested by growth curve analysis (Fig. 1).

Cell viability. The viable cell fractions in 37°C samples increased from 41% ($\pm 6.5\%$ SE; $n = 10$) at day 0.8 to 59% ($\pm 17.8\%$ SE; $n = 10$) at day 1.8 (Fig. 2). The total cell count peaked after 3.7 days (OD_{600} of ~ 2), but the viable cell fraction did not show any significant increase, with only 60% ($\pm 11.2\%$ SE; $n = 10$) of total cells recorded as being viable at that point. At 15°C , however, a lower total cell count on day 7 was not reflective of the viable cell fraction, which was 79% ($\pm 13.8\%$ SE; $n = 10$) (Fig. 2). This trend continued, as recorded at 17.2 days with 84% ($\pm 9.65\%$ SE; $n = 10$) of cells being identified as viable. After this observed period of

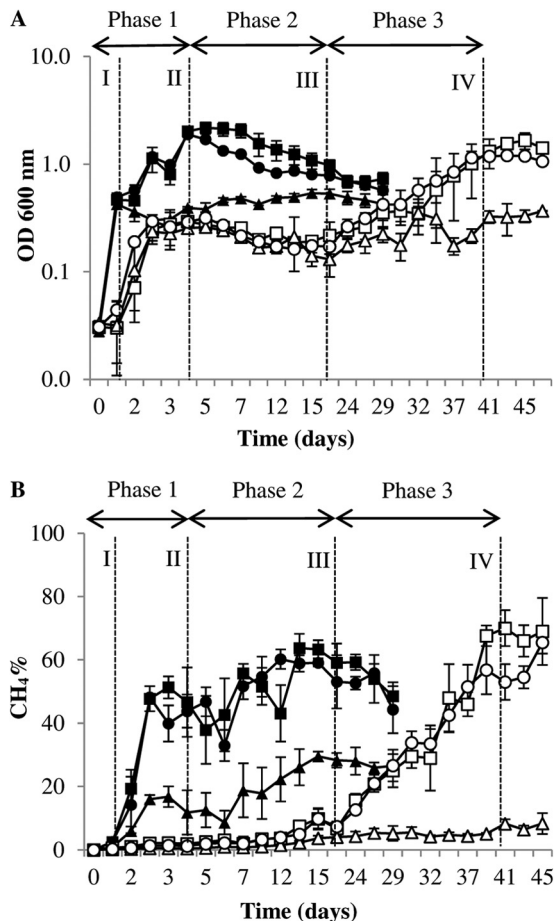


FIG 1 Growth profiles of *M. barkeri* incubated at 37°C and 15°C. Optical density (at 600 nm) measurements (A) and percent CH₄ headspace measurements (B) were determined in tandem for *M. barkeri* grown at 37°C with H₂/CO₂ plus methanol ■, methanol alone ●, and H₂/CO₂ alone ▲ and at 15°C with H₂/CO₂ plus methanol □, methanol alone ○, and H₂/CO₂ alone △. Error bars indicate the standard deviations and are the result of at least three replicates. Data represent phase 1 (samples I and II), phase 2 (sample III), and phase 3 (sample IV) of the LTAS experiment.

minimal growth but high viability, the total cell counts increased in 15°C samples, while the viable fraction decreased to 66% ($\pm 9.5\%$ SE; $n = 10$) on day 37. The spatial arrangement of *M. barkeri* aggregates from both temperatures varied, with 37°C samples consisting of layered branching aggregates while the 15°C aggregates were more consistent in size, with clusters rarely exceeding 10 μm in diameter (Fig. 2).

Proteomics analysis. In order to gain some insight into the low-temperature adaptation of *M. barkeri*, two iTRAQ experiments were performed, one involving cultures grown at 37°C and exposed to a temperature drop to 15°C (LTSR) and another experiment involving cultures grown at 15°C (LTAS). In the LTSR study, a total of 127 proteins ($P \leq 0.05$) were detected in both 37°C and 15°C samples. From these, 20 proteins (16%) were found to be differentially expressed as a function of temperature by a 1.5-fold change or more (Table 3). Among these proteins, various functional categories were evident. Two proteins involved in CO₂ methanogenesis were detected at higher levels at 37°C than at 15°C (Mbar_A1095 and Mbar_A1763) (Table 3). Methanogenesis from

dimethylamine and methanol showed contrasting results, with a protein involved in the dimethylamine pathway (Mbar_A3605) identified at a higher level in the 37°C sample, while the corrinoid protein involved in the methanol pathway (Mbar_A3637) was up-regulated at 15°C. Several information-processing enzymes were identified as being differentially expressed. These included an XRE domain protein (Mbar_A1033), which plays a key role in DNA binding (41), and an elongation factor 2 (EF-2) protein (Mbar_A3686), both of which were upregulated at 15°C (Table 3). In addition, a ribosomal protein (Mbar_A0614) was found to be expressed at a higher level at 15°C. Also, several stress proteins were upregulated at 37°C, including a heat shock protein (Mbar_A1543) and two subunits of the thermosome (Ths) protein (Mbar_A1084 and Mbar_A1201) (Table 3).

In conjunction with the *M. barkeri* growth profile at 15°C, the iTRAQ samples for the LTAS study were taken during the three phases observed: phase 1 (initial adaptation [samples I and II]), phase 2 (stationary phase [sample III]), and phase 3 (primary growth phase [sample IV]) (Fig. 1 and Table 1). In total, 104 proteins ($P \leq 0.05$) were identified in all samples, with 41 (39%) found to be differentially expressed (1.5-fold difference) between two or more samples (Table 3).

Figure 3 illustrates differentially expressed protein profiles for each of the phases investigated in the LTAS study. Proteins relating to CO₂ and methanol methanogenesis as well as methylamine-specific proteins were found to be significantly expressed in one or more of these phases. A methanol metabolism protein (Mbar_A1063) was upregulated in phase 1 and phase 2 samples in comparison to the phase 3 sample. A trimethylamine protein (Mbar_A1502) was found to be expressed at a higher level in the phase 2 sample than in other samples. However, the majority of significantly expressed methanogenesis proteins were upregulated in the phase 3 sample (Fig. 3; Table 3).

Four proteins relating to transcription and translation were upregulated in phase 2 and phase 3 samples compared with phase 1 samples (Table 3). These included a protein involved in transcriptional RNA synthesis (Mbar_A2536) and a protein biosynthesis catalyst (Mbar_A3685). However, the EF-2 protein (Mbar_A3686) as well as a transcriptional regulator (Mbar_A1033) was found to be upregulated in phase 1 and phase 2 samples compared with the phase 3 sample level (Table 3). This result was consistent with the LTSR study in which both of these proteins were detected at higher levels at 15°C, suggesting that they might be important for *M. barkeri* during initial stages of low-temperature adaptation. Two other DNA binding and repair proteins were found to be upregulated in phase 2 and phase 3 samples compared to phase 1 samples. These included a DNA regulator (Mbar_A1584) involved in transcription (42). General metabo-

TABLE 2 Maximum specific growth rates of *M. barkeri*

Substrate	Temp (°C)	μ_{max} (day ⁻¹) ^a	% Decrease in μ_{max}	Generation time (days)
H ₂ /CO ₂ + methanol	37	0.5 \pm 0.03	0	1.4
Methanol	37	0.46 \pm 0.06	8	1.5
H ₂ /CO ₂	37	0.11 \pm 0.02	78	6.3
H ₂ /CO ₂ + methanol	15	0.12 \pm 0.07	0	6.2
Methanol	15	0.09 \pm 0.03	25	10.7
H ₂ /CO ₂	15	0.03 \pm 0.09	75	24.2

^a Values are means \pm SD ($n = 3$). μ_{max} , maximum specific growth rate (1/days).

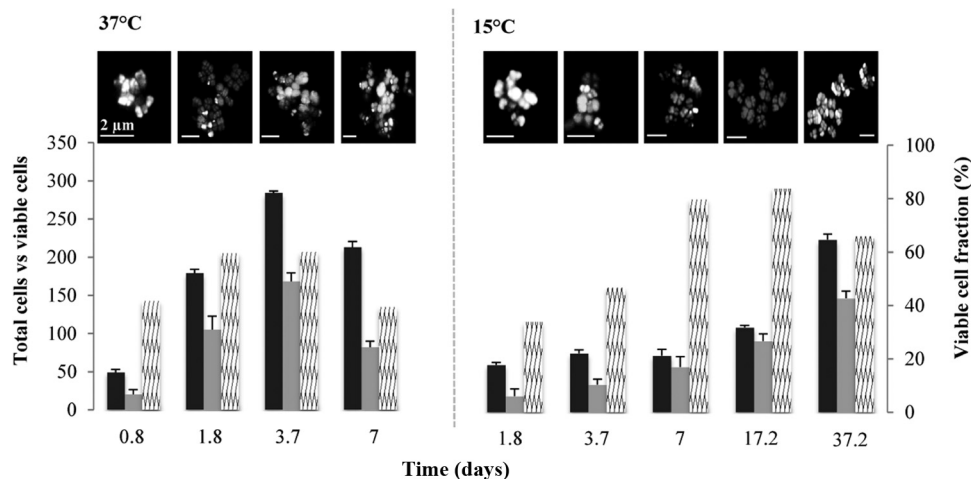


FIG 2 Cell viability of *M. barkeri* grown at 37°C and 15°C. Bar charts represent total cell counts (black bars), viable cell counts (gray bars), and the viable fraction (%) of total cell counts (hatched bars). Representative images from live/dead staining of *M. barkeri* taken from samples during the course of the growth curve incubations are shown above the graphs. Error bars indicate the standard deviations and are the result of at least three replicates.

lism proteins identified in the LTAS study were found to be involved in diverse pathways, including amino acid and vitamin biosynthesis, glycolysis, and electron transport (Table 3). Six of these proteins, which included an oxidoreductase protein (Mbar_A2189) essential in glycolysis and biosynthesis of secondary metabolites, were expressed at higher levels in the phase 3 sample than in the phase 1 samples.

Proteins involved in oxidative stress, protein folding, and proteolysis were also represented in the LTAS data set (Table 3). Two thermosome proteins (Mbar_A1084 and Mbar_A1201) were upregulated in the phase 3 sample compared with phase 1 sample levels, and this was also the case for a universal stress protein (Mbar_A0825) (Fig. 3). Also, a peptidyl prolyl isomerase (Mbar_A2249) was upregulated in the phase 2 sample compared to levels in other samples. Although little is known regarding chaperone-like activity of the peptidyl prolyl isomerase, a study on *Methanococcoides burtonii* reported the upregulation of this protein when the organism was grown at 4°C compared to 26°C (43), therefore suggesting that this protein may play an important role in low-temperature adaptation of *M. barkeri*. Finally, a DnaK heat shock protein (Mbar_A3433) was found to be upregulated in phase 2, and a proteolysis protein (Mbar_A2503) was found to be upregulated in the phase 3 sample compared to phase 1 samples (Fig. 3 and Table 3).

In order to complement the iTRAQ results, 2-DGE was undertaken on *M. barkeri* samples grown at 37°C and 15°C (LTAS study). These samples were taken at time points with similar OD₆₀₀ and percent CH₄ levels for each temperature (Table 1). An average of 179 (standard deviation [SD], 18.4; $n = 6$) reproducible protein spots were detected on 2-D gels, from which 79 (44%) were found to be upregulated at 37°C while 39 (22%) proteins were upregulated at 15°C, and 61 (34%) were conserved for each temperature. Two proteins representing differential expression for each temperature were excised and identified using nLC-ESI-MS/MS. The universal stress protein (Mbar_A0825) was found to be upregulated (up 4.5-fold) at 37°C, while a proteasome (Mbar_A2503) was expressed at a higher level in the 15°C sample (up 2.9-fold) (Fig. 4). In the LTSR iTRAQ experiment, the univer-

sal stress protein was upregulated at 37°C while the proteasome was upregulated at 15°C, thus showing consistency between the two proteomic techniques applied (Table 3). A protein responsible for methyl-coenzyme M reduction (Mbar_A0893) was conserved for each temperature, which was in agreement with the LTSR iTRAQ experiment.

DISCUSSION

The low-temperature adaptation of *M. barkeri* was investigated through two experimental approaches: (i) low-temperature shock response (LTSR) and (ii) low-temperature adaptation strategy (LTAS). In the LTSR experiment, we applied an iTRAQ method to characterize the protein expression profile of *M. barkeri* before and after a temperature drop from 37°C to 15°C. In the LTAS experiment, *M. barkeri* growth at 15°C was characterized through proteomic samples taken at specific time points to coincide with a particular phase of growth. Also, cell viability measurements were recorded in the LTAS experiment, which included measurements at the proteomics sampling time points, in order to give a concise overview of the submesophilic growth capacity of *M. barkeri*. For the LTSR experiment, a total of 20 (13%) proteins were found to be upregulated at either 37°C or 15°C, while in the LTAS experiment there were 43 (41%) proteins found to be differentially expressed during incubation at 15°C (Table 3). Overall, this study provided new insights into the low-temperature adaptation capacity of *M. barkeri*.

Methanogenesis from methanol was found to be significant for *M. barkeri* at 15°C, with corrinoid protein upregulation (Mbar_A3637) at 2.8-fold at this low temperature compared with 37°C (LTSR). During growth at 15°C (LTAS), two methanol metabolism proteins (Mbar_A1063 and Mbar_A1064) were found to be upregulated at different time points. Taken together, these results indicate the ability of *M. barkeri* to efficiently utilize methanol under submesophilic conditions. Two proteins involved in H₂/CO₂ metabolism proteins were found to be upregulated at 37°C (Mbar_A1095, up 3.3-fold; Mbar_A1763, up 3.2-fold), which might suggest a preference for H₂/CO₂ at mesophilic temperatures. The pathway involved in trimethylamine and dim-

TABLE 3 Differentially expressed proteins from iTRAQ experiments

Gene function and locus	Protein ^b	Sequence coverage (%)	Protein expression ratio ^a					
			LTSR (37°C/15°C)	P1 vs P2		P1 vs P3		P2 vs P3 (III/IV)
				I/III	II/III	I/IV	II/IV	
Methanogenesis genes								
CO ₂ specific								
Mbar_A0450	Coenzyme F ₄₂₀ hydrogenase subunit G (FrhG)	12		0.65	0.62	0.51	0.68	NS
Mono/di/trimethylamine specific								
Mbar_A0841	Methylcobalamin:CoM methyltransferase (MtbA)	8	NS	0.67	0.62	0.55	0.51	NS
Mbar_A3605	Dimethylamine methyltransferase (MtbB)	8	3	0.68	0.63	0.56	0.42	NS
Mbar_A1502	Trimethylamine methyltransferase (MtbB)	7	NS	0.48	0.54	0.57	0.62	1.54
Methanol specific								
Mbar_A1063	Methanol corrinoid protein (MtaC)	30	NS	NS	NS	0.45	0.44	0.64
Mbar_A3637	Methanol corrinoid protein (MtaC)	12	0.3					
Mbar_A1064	Methanol:corrinoid methyltransferase (MtaB)	17	NS	NS	NS	1.62	1.69	1.62
Common								
Mbar_A1095	F ₄₂₀ -dependent H ₄ MPT dehydrogenase (Mtd)	34	3.3	NS	NS	0.67	0.62	0.62
Mbar_A1763	Formylmethanofuran dehydrogenase subunit B (FwdB)	13	3.2					
Mbar_A0893	Methyl-coenzyme reductase subunit A (McrA)	18	NS	NS	NS	0.51	0.57	0.56
Mbar_A1182	Methyl-coenzyme reductase subunit B (McrB)	15	NS	NS	NS	0.65	0.55	0.43
Mbar_A1256	Tetrahydromethanopterin S-methyltransferase subunit G (MtrG)	26	4.8	NS	NS	NS	NS	NS
Cellular information processing genes								
Transcription								
Mbar_A2536	Putative nickel-responsive regulator 1 (NikR)	29	2.7	NS	NS	NS	0.61	0.64
	DNA-directed RNA polymerase I, II and III, 7.3-kDa polypeptide	37		0.56	0.52	0.47	0.45	NS
Translation								
Mbar_A3687	30S ribosomal protein S7P (RpsG)	27		1.78	1.65	1.56	NS	NS
Mbar_A1149	30S ribosomal protein S17 (Rps17E)	16		NS	NS	1.83	1.56	1.64
Mbar_A3231	50S ribosomal protein L21E (Rpl21)	15		0.69	0.54	0.56	0.33	NS
Mbar_A0614	50S ribosomal protein L11P (RplA)	16	0.3	NS	NS	0.68	0.64	0.65
Mbar_A3173	Aspartyl-tRNA synthetase (AspS)	23	NS	1.66	1.99	NS	NS	0.45
Mbar_A0454	SSU ribosomal protein S19E (Rps19)	4	NS	0.72	0.64	0.55	0.53	NS
Mbar_A0623	Isocitrate dehydrogenase (Idh1)	4	NS	NS	NS	0.55	0.51	NS
Mbar_A2048	Leucyl-tRNA synthase (LeuS)	17	2.6					
Mbar_A3685	Elongation factor 1 subunit A (EF1A)	12	NS	0.78	0.67	0.69	0.63	NS
Mbar_A3686	Elongation factor 2 (EF-2)	18	0.5	NS	NS	1.61	1.50	1.63
DNA binding and repair								
Mbar_A1033	Transcriptional regulator, XRE family	8	0.3	NS	NS	1.59	1.52	1.54
Mbar_A1182	Nucleoid protein (MC1)	22		0.63	0.53	0.49	0.35	NS
Mbar_A1584	Archaeal histone (HmbA)	30		0.62	0.56	0.50	0.54	NS
General metabolism genes								
Amino acid biosynthesis								
Mbar_A0248	3-Isopropylmalate dehydrogenase (AfkS)	7	1.92	0.51	0.52	0.41	0.41	NS
Mbar_A0220	Ketol-acid reductoisomerase (IlvC)	9	1.78	0.54	NS	0.62	0.58	NS
Mbar_A1431	D-3-Phosphoglycerate dehydrogenase (PhgdH)	37	2.17	NS	NS	NS	NS	NS
Mbar_A1094	Phosphoserine phosphatase (PspH)	18	1.84	NS	NS	NS	NS	NS
Mbar_A3623	Tryptophan synthase alpha chain 1 (ThiC)	12	3.19					
Vitamin biosynthesis								
Mbar_A0597	Phosphomethylpyrimidine synthase 1 (TrpA)	10	1.66	NS	0.66	NS	NS	NS
Mbar_A1056	CobW protein	4		NS	0.54	NS	NS	NS
Glycolysis and energy metabolism								
Mbar_A2189	Glyceraldehyde-3-phosphate dehydrogenase (Gap2)	6	NS	NS	NS	0.53	0.49	NS
Mbar_A0392	H ⁺ -transporting ATP synthase (NtpE)	19	NS	NS	NS	0.47	0.44	0.66
Electron transport								
Mbar_A1847	Methanophenazine-reducing hydrogenase	8	NS	0.61	NS	0.42	0.46	NS
Mbar_A3651	HesB protein	13	NS	0.63	0.61	0.41	0.43	0.65
Chaperones and stress proteins								
Mbar_A1084	Themosome subunit A (Hsp60)	22	2.67	0.62	NS	0.51	0.48	0.57
Mbar_A1201	Themosome subunit B (Hsp60)	15	1.54	NS	NS	0.52	0.52	0.66

(Continued on following page)

TABLE 3 (Continued)

Gene function and locus	Protein ^b	Sequence coverage (%)	LTSR (37°C/15°C)	Protein expression ratio ^a				
				P1 vs P2		P1 vs P3		P2 vs P3
				I/III	II/III	I/IV	II/IV	(III/IV)
Mbar_A3433	Chaperone protein (DnaK)	8	NS	0.56	0.55	NS	NS	1.56
Mbar_A1543	60-kDa chaperone (GroEL)	32	1.67					
Mbar_A2503	Proteasome subunit A (PrcA)	12	NS	0.56	0.53	0.47	0.44	NS
Mbar_A2249	Peptidyl-prolyl isomerase (SlyD)	20	NS	0.45	0.42	NS	NS	1.64
Mbar_A0213	Prefoldin subunit B (PrcA)	21	NS	1.56	NS	NS	NS	NS
Mbar_A0825	Universal stress protein	11	3.24	NS	NS	0.46	0.45	1.66
Unknown-function genes								
Mbar_A0488	Putative uncharacterized protein	8	NS	0.52	0.64	0.53	0.61	NS
Mbar_A1026	Putative uncharacterized protein	29		NS	NS	1.57	1.51	1.67
Mbar_A0376	Putative uncharacterized protein	17		NS	NS	0.57	0.51	0.64
Mbar_A1027	Putative uncharacterized protein	46		1.53	1.56	2.38	2.45	2.12
Mbar_A3219	Putative uncharacterized protein	15		NS	NS	0.41	0.43	NS

^a For the LTSR experiment, the ratios represent values for growth at 37°C versus growth at 15°C (37°C/15°C). For the LTAS experiment, the ratios represent the values for the indicated sample(s) within phases 1 (P1, samples I and II), 2 (P2, sample III), and 3 (P3, sample IV). NS, no statistically significant difference. All samples were fed methanol plus H₂/CO₂.

^b CoM, coenzyme M; SSU, small subunit; H₄MPT, tetrahydromethanopterin.

ethylamine metabolism was found to be active in *M. barkeri* during growth at 15°C. Interestingly, a methyltransferase protein (Mbar_A1502), which catalyzes trimethylamine reduction to methyl-coenzyme M, was upregulated during the stationary

phase compared to other stages of growth (Table 3). Thus, the ability to undertake methylamine methanogenesis at 15°C may confer an advantage for *M. barkeri* survival in a low-temperature environment.

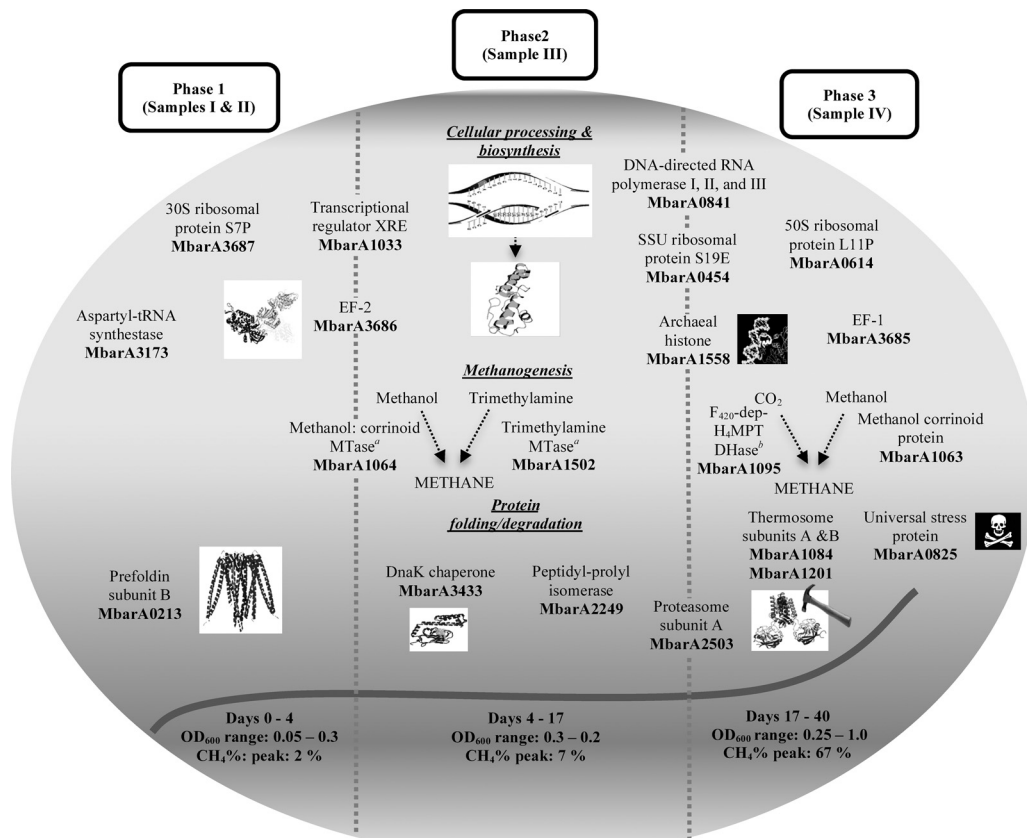


FIG 3 Differentially expressed proteins at specific phases of *M. barkeri* growth at 15°C are shown. Proteins located on broken lines represent a conserved result between particular phases. MTase, methyltransferase; SSU, small subunit; F₄₂₀-dep-H₄MPT DHase, F₄₂₀-dependent methylenetetrahydromethanopterin dehydrogenase.

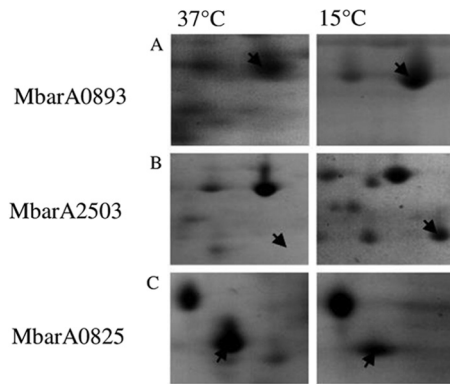


FIG 4 2-DGE gel sections comprising proteins extracted from *M. barkeri* grown at 37°C and 15°C. (A) Methyl-coenzyme M reductase subunit G protein (Mbar_A0893) conserved for each temperature (expression level at 37°C/expression level at 15°C, up 1.24-fold). (B) Proteasome subunit A (Mbar_A2503) upregulated at 15°C (expression level at 15°C/expression level at 37°C, up 2.87-fold). (C) Universal stress protein (Mbar_A0825) upregulated at 37°C (expression level at 37°C/expression level at 15°C, up 3.81-fold).

Proteins involved in translation were detected in both iTRAQ experiments. The EF-2 protein (Mbar_A3686) was upregulated at 15°C compared to 37°C (LTAS), and, furthermore, it was found to be upregulated in the initial phases of growth at 15°C (LTAS) (phase 1 and phase 2 samples compared to phase 3 sample) (Fig. 3). Therefore, this protein may play a role in the initial stages of low-temperature adaptation in *M. barkeri*. The EF-2 protein has been the focus in many studies relating to *Methanococcoides burtonii*, a psychrotolerant methanogen isolated from Ace Lake, Antarctica (44–46). It has been suggested that the low stability of EF-2 (e.g., fewer salt bridges) facilitates high enzymatic activity during growth of *M. burtonii* at low temperatures. Therefore, it is conceivable that EF-2 may also confer an advantage in *M. barkeri* during submesophilic growth. The importance of low-temperature DNA binding and repair was evident through the upregulation of the XRE transcriptional regulator (Mbar_A1033) as well as two other DNA binding proteins found at 15°C.

Cellular chaperone proteins were predominant at 37°C. A chaperonin protein (Mbar_A1543) was upregulated at 37°C (LTAS), which relates to a previous study where a corresponding RNA transcript was upregulated under heat stress conditions (47). In addition to this, a thermosome (Ths) protein was found to be upregulated at 37°C (LTAS) (Table 3). The Ths protein was also found to be upregulated in the latter phase of growth at 15°C (LTAS, phase 3) (Fig. 3), suggesting an important functional role under submesophilic exponential growth conditions. A DnaK chaperone (Mbar_A3433), which was found to be upregulated during stationary-phase growth at 15°C (LTAS, phase 2) (Fig. 3), has been reported to play an important role in cell survival under cell stress conditions (48), particularly heat stress (49). The recombinant expression of DnaK from the psychrophilic *Shewanella* sp. in *Escherichia coli* was found to confer the ability to grow at 15°C to an *E. coli* mutant strain (50). Together with a peptidyl propyl isomerase (Mbar_A2249), these proteins are important for low-temperature adaptation in *M. barkeri* and require further examination to characterize their respective roles in more detail.

Cell viability measurements recorded during growth of *M.*

barkeri at 15°C (LTAS) gave insights into the capacity of this methanogen to survive under submesophilic conditions. This was highlighted with *M. barkeri* cells showing 83% ($\pm 9.65\%$ SE; $n = 10$) cell viability after 17 days of incubation at 15°C. It is at this point (end of phase 2) of incubation that viable *M. barkeri* cells (only cultures with methanol) exhibited complete adaptation to cold conditions as shortly after this sampling point the primary growth phase was recorded, corresponding to OD₆₀₀ and percent CH₄ readings reaching comparable levels to those of the 37°C samples (exponential phase). Together with proteomic data, these findings contribute to a better understanding of *Methanosarcina* survival in low-temperature environments, e.g., EF-2-mediated protein synthesis and chaperone activity (DnaK/proteasome system) facilitating psychrophilic adaptation.

It is conceivable that *Methanosarcina* spp. utilize substrates other than acetate in well-functioning LTAS applications, which in turn may offer a favorable advantage through bypassing direct substrate competition. If an alternative metabolic route was accessible in LTAD, such as C₁ metabolism, this might promote the survival of *Methanosarcina* spp. (possibly in a long lag phase observed in phase 2 of the LTAS experiment). Acetate accumulation brought about through a perturbation event, such as after a temperature drop, may then provide *Methanosarcina* with enough substrate to accumulate above the threshold value (>1 mM), which was evident in previous low-temperature (14) and high-temperature (51) anaerobic digestion studies. Targeted functional approaches are required to uncover the metabolic and adaptation strategies of *Methanosarcina* spp. in a mixed community context. The application of a polyphasic experimental design would be ideal, combining, for example, DNA quantification and proteomics methods with isotope labeling studies (e.g., separate incubations with ¹⁴C-labeled methanol, H₂/CO₂, and acetate). Together, these approaches may shine some light on the functional role of this methanogen in LTAD systems.

In a process context, procuring a psychrophilic seed biomass in future LTAD applications may not be required for studies characterizing the psychrotolerant capabilities of methanogens and other microbial groups underpinning mesophilic seed biomass. In addition to this, bioreactor design and operation can be directed away from a performance-related paradigm, where differences between successful and unsuccessful bioreactor trials are still poorly understood. Instead, community-based approaches may be undertaken, e.g., system-based mathematical modeling.

ACKNOWLEDGMENTS

We are grateful to colleagues in the Microbial Ecology Lab and in Microbiology at the National University of Ireland, Galway, for all the help given in preparation of the manuscript.

We thank the Wellcome Trust for funding mass spectrometry equipment at the University of St. Andrews. This research was financially supported by Science Foundation Ireland (grants RFP 08/RFP/EOB1343 and 06/CP/E006).

REFERENCES

- Church MJ, DeLong EF, Ducklow HW, Karner MB, Preston CM, Karl DM. 2003. Abundance and distribution of planktonic archaea and bacteria in the waters west of the Antarctic peninsula. *Limnol. Oceanogr.* 48:1893–1902.
- Galand PE, Lovejoy C, Vincent WF. 2006. Remarkably diverse and contrasting archaeal communities in a large arctic river and the coastal Arctic Ocean. *Aquat. Microb. Ecol.* 44:115–126.
- Pernthaler J, Glockner FO, Unterholzner S, Alfreider A, Psenner R,

- Amann R. 1998. Seasonal community and population dynamics of pelagic bacteria and archaea in a high mountain lake. *Appl. Environ. Microbiol.* 64:4299–4306.
4. Wagner D, Kobabe S, Pfeiffer EM, Hubberten HW. 2003. Microbial controls on methane fluxes from a polygonal tundra of the Lena Delta, Siberia. *Permafrost Periglac. Process.* 14:173–185.
 5. Battin TJ, Willie A, Sattler B, Psenner R. 2001. Phylogenetic and functional heterogeneity of sediment biofilms along environmental gradients in a glacial stream. *Appl. Environ. Microbiol.* 67:799–807.
 6. Cavicchioli R. 2006. Cold adapted archaea. *Nat. Rev. Microbiol.* 4:331–343.
 7. Hoj L, Olsen RA, Torsvik VL. 2008. Effects of temperature on the diversity and community structure of known methanogenic groups and other archaea in high Arctic peat. *ISME J.* 2:37–48.
 8. Morozova D, Wagner D. 2007. Highly resistant methanogenic archaea from Siberian permafrost as candidates for the possible life on Mars. *Int. J. Astrobiol.* 6:59–87.
 9. Collins G, Enright AM, Scully C, Mahony T, O'Flaherty V. 2006. Application and biomolecular monitoring of psychrophilic anaerobic digestion. *Water Sci. Technol.* 54:41–47.
 10. Connaughton S, Collins G, O'Flaherty V. 2006. Psychrophilic and mesophilic anaerobic digestion of brewery effluent: a comparative study. *Water Res.* 40:2503–2510.
 11. O'Reilly J, Lee C, Collins G, Chinalia FA, Mahony T, O'Flaherty V. 2009. Quantitative and qualitative analysis of methanogenic communities in mesophilically and psychrophilically cultivated anaerobic granular biofilms. *Water Res.* 43:3365–3374.
 12. McHugh S, Carton M, Collins G, O'Flaherty V. 2004. Reactor performance and microbial community dynamics during anaerobic biological treatment of wastewater at 16–37°C. *FEMS Microbiol. Ecol.* 48:369–378.
 13. McHugh S, Collins G, O'Flaherty V. 2006. Long-term, high-rate anaerobic biological treatment of whey wastewaters at psychrophilic temperatures. *Bioresour. Technol.* 97:1669–1678.
 14. McKeown R, Scully C, Enright AM, Chinalia FA, Lee C, Mahony T, Collins G, O'Flaherty V. 2009. Psychrophilic methanogenic community development during long-term cultivation of anaerobic granular biofilms. *ISME J.* 3:1231–1242.
 15. Zhu J, Zheng H, Guomin A, Zhang G, Liu D, Xiaoli L, Dong X. 2012. The genome characteristics and predicted function of methyl-group oxidation pathway in the obligate acetoclastic methanogens, *Methanosaeta* spp. *PLoS One* 7:e36756. doi:10.1371/journal.pone.0036756.
 16. Mori K, Lino T, Suzuki Yamaguchi K-IK, Kamagata Y. 2012. Acetoclastic and NaCl-requiring methanogen "*Methanosaeta pelagica*" sp. nov., isolated from marine tidal flat sediment. *Appl. Environ. Microbiol.* 78:3416–3423.
 17. Fey A, Conrad R. 2000. Effect of temperature on carbon and electron flow and on the archaeal community in methanogenic rice field soil. *Appl. Environ. Microbiol.* 66:4790–4797.
 18. Griffin ME, McMahon KD, Mackie RI, Raskin L. 1998. Methanogenic population dynamics during start-up of anaerobic digesters treating municipal solid waste and biosolids. *Biotechnol. Bioeng.* 57:342–355.
 19. Collins G, Mahony T, O'Flaherty V. 2006. Stability and reproducibility of low-temperature anaerobic biological wastewater treatment. *FEMS Microbiol. Ecol.* 55:449–458.
 20. Diaz EE, Stams AJ, Amils R, Sanz JL. 2006. Phenotypic properties and microbial diversity of methanogenic granules from a full-scale upflow anaerobic sludge bed reactor treating brewery wastewater. *Appl. Environ. Microbiol.* 72:4942–4949.
 21. Liu Y, Xu H, Show K, Tay J. 2002. Anaerobic granulation technology for wastewater treatment. *J. Microbiol. Biotechnol.* 18:99–113.
 22. Siggins A, Enright AM, O'Flaherty V. 2011. Low-temperature (7°C) anaerobic treatment of a trichloroethylene-contaminated wastewater: microbial community development. *Water Res.* 45:4035–4046.
 23. Siggins A, Enright AM, O'Flaherty V. 2011. Methanogenic community development in anaerobic granular bioreactors treating trichloroethylene (TCE)-contaminated wastewater at 37°C and 15°C. *Water Res.* 45:2452–2462.
 24. O'Reilly J, Lee C, Chinalia FA, Collins G, Mahony T, O'Flaherty V. 2010. Microbial community dynamics associated with biomass granulation in low-temperature (15°C) anaerobic wastewater treatment bioreactors. *Bioresour. Technol.* 101:6336–6344.
 25. McKeown RM, Scully C, Mahony T, Collins G, O'Flaherty V. 2009. Long-term (1243 days), low-temperature (4–15°C), anaerobic biotreatment of acidified wastewaters: bioprocess performance and physiological characteristics. *Water Res.* 43:1611–1620.
 26. Bock AK, Schonheit P. 1995. Growth of *Methanosarcina barkeri* (Fusaro) under nonmethanogenic conditions by the fermentation of pyruvate to acetate: ATP synthesis via the mechanism of substrate level phosphorylation. *J. Bacteriol.* 177:2002–2007.
 27. Mazumder TK, Nishio N, Fukuzaki S, Nagai S. 1986. Effect of sulfur-containing compounds on growth of *Methanosarcina barkeri* in defined medium. *Appl. Environ. Microbiol.* 52:617–622.
 28. Muller V, Blaut M, Gottschalk G. 1986. Utilization of methanol plus hydrogen by *Methanosarcina barkeri* for methanogenesis and growth. *Appl. Environ. Microbiol.* 52:269–274.
 29. Feist AM, Scholten JCM, Palsson BO, Brockman FJ, Ideker T. 2006. Modelling methanogenesis with a genome-scale metabolic reconstruction of *Methanosarcina barkeri*. *Mol. Syst. Biol.* 2:2006.0004. doi:10.1038/msb4100046.
 30. Maeder DL, Anderson I, Brettin TS, Bruce DC, Gilna P, Han CS, Lapidus A, Metcalf WM, Saunders E, Tapia R, Sowers KR. 2006. The *Methanosarcina barkeri* genome: comparative analysis with *Methanosarcina acetivorans* and *Methanosarcina mazei* reveals extensive rearrangement within methanosarcinal genomes. *J. Bacteriol.* 188:7922–7931.
 31. Buchenau B, Thauer RK. 2004. Tetrahydrofolate-specific enzymes in *Methanosarcina barkeri* and growth dependence of this methanogenic archaeon on folic acid or p-aminobenzoic acid. *Arch. Microbiol.* 182:313–325.
 32. Goenrich M, Duin EC, Mahlert F, Thauer RK. 2005. Temperature dependence of methyl-coenzyme M reductase activity and of the formation of the methyl-coenzyme M reductase red2 state induced by coenzyme B. *J. Biol. Inorg. Chem.* 10:333–342.
 33. Nomura T, Nagao T, Yoshihara A, Tokumoto H, Konishi Y. 2006. Selective immobilization of acetoclastic methanogens to support material. *J. Soc. Powder Technol. Jpn.* 43:653–659. (In Japanese.)
 34. Clesceri LS, Greenberg AE, Eaton AD (ed). 1998. Standard methods for the examination of water and wastewater, 19th ed. American Public Health Association, Washington, DC.
 35. Hao X, Wang Q, Zhang X, Cao Y, van Loosdrecht MCM. 2009. Experimental evaluation of decrease in bacterial activity due to cell death and activity decay in activated sludge. *Water Res.* 43:3604–3612.
 36. Abram F, Enright AM, O'Reilly J, Botting CH, Collins G, O'Flaherty V. 2011. A metaproteomic approach gives functional insights into anaerobic digestion. *J. Appl. Microbiol.* 110:1550–1560.
 37. Gozal D, Jortani S, Ayelet BS, Kheirandish-Gozal L, Bhattacharjee R, Kim J, Capdevilla S. 2009. Two-dimensional differential in-gel electrophoresis proteomic approaches reveal urine candidate biomarkers in pediatric obstructive sleep apnea. *Am. J. Respir. Care Med.* 180:1253–1261.
 38. Zhang G, Spellman DS, Skolink EY, Neubert TA. 2006. Quantitative phosphotyrosine proteomics of EphB2 signaling by stable isotope labeling with amino acids in cell culture (SILAC). *J. Proteome Res.* 5:581–588.
 39. Shilova IV, Seymour SL, Patel AA, Loboda A, Tang WH, Keating SP, Hunter CL, Nuwaysir LM, Schaeffer DA. 2007. The paragon algorithm, a next generation search engine that uses sequence temperature values and feature probabilities to identify peptides from tandem mass spectra. *Mol. Cell. Proteomics* 6:1638–1655.
 40. Rittmann BE. 2007. The membrane biofilm reactor is a versatile platform for water and wastewater treatment. *Environ. Eng. Res.* 12:157–175.
 41. Veit K, Ehlers C, Ehrereich A, Salmon K, Hovey R, Gunsalus RP, Deppenmeier U, Schmitz RA. 2006. Global transcriptional analysis of *Methanosarcina mazei* strain Gö1 under different nitrogen availabilities. *Mol. Genet. Genomics* 276:41–55.
 42. Weidenbach K, Ehlers C, Kock J, Ehrenreich A, Schmitz RA. 2008. Insights into the NrpR regulon in *Methanosarcina mazei* Gö1. *Arch. Microbiol.* 190:319–332.
 43. Goodchild A, Raftery M, Saunders NF, Guilhaus M, Cavicchioli R. 2005. Cold adaptation of the Antarctic archaeon, *Methanococoides burtonii* assessed by proteomics using ICAT. *J. Proteome Res.* 4:473–480.
 44. Gu J, Hilser VJ. 2009. Sequence-based analysis of protein energy landscapes reveals nonuniform thermal adaptation within the proteome. *Mol. Biol. Evol.* 26:2217–2227.
 45. Siddiqui KS, Cavicchioli R, Thomas T. 2002. Thermodynamic activation

- properties of elongation factor 2 (EF-2) proteins from psychrotolerant and thermophilic *Archaea*. *Extremophiles* 6:143–150.
46. Thomas T, Cavicchioli R. 2000. Effect of temperature on stability and activity of elongation factor 2 proteins from Antarctic and thermophilic methanogens. *J. Bacteriol.* 182:1328–1332.
 47. Zhang W, Culley DE, Brockman FL. 2006. DNA microarray analysis of anaerobic *Methanosarcina barkeri* reveals responses to heat shock and air exposure. *J. Ind. Microbiol. Biotechnol.* 33:784–790.
 48. Clarens M, Macario AJ, Conway de Marcario E. 1995. The archaeal *dnaK-dnaJ* gene cluster: organisation and expression in the methanogen *Methanosarcina mazei*. *J. Mol. Biol.* 250:191–201.
 49. De Biase A, Marcario AJ, Conway de Marcario E. 2002. Effect of heat stress on promoter binding by transcription factors in the cytosol of the archaeon *Methanosarcina mazei*. *Gene* 282:189–197.
 50. Yoshimune K, Galkin A, Kulalova L, Yoshimura T, Esaki N. 2005. Cold-active DnaK of an Antarctic psychrotroph *Shewanella* sp. Ac10 supporting the growth of *dnaK*-null mutant of *Escherichia coli* at cold temperatures. *Extremophiles* 9:145–150.
 51. Hori T, Haruta S, Ueno Y, Ishii M, Igarashi Y. 2006. Dynamic transition of a methanogenic population in response to the concentration of volatile fatty acids in a thermophilic anaerobic digester. *Appl. Environ. Microbiol.* 72:1623–1630.